

Competing Structural Reaction Mechanisms in the Topotactic Dehydration of $\text{KVO}_3 \cdot \text{H}_2\text{O}$ and Their Geometrical Interpretation

J. R. GÜNTER,¹ R. BISCHOF, AND H. R. OSWALD

*Institute for Inorganic Chemistry, University of Zürich,
Winterthurerstrasse 190, CH-8057 Zürich, Switzerland*

Received August 18, 1981

It is shown that the dehydration of $\text{KVO}_3 \cdot \text{H}_2\text{O}$ to KVO_3 occurs in a topotactic manner, but that several geometrical reaction mechanisms compete. Three of these consist of an elongation of essentially preserved anionic vanadate chains by over 50% (combined with chain rotation), thus reducing the required number of strong bonds to be broken to a minimum, whereas the other two can be explained by a reconstruction of the chains within well-defined lattice planes, needing a larger number of breaking bonds, but minimizing the need of atomic displacements. By geometrical arguments the occurrence of additional product orientations can be ruled out. The influence of the reaction conditions on the kind of mechanism to occur is tentatively described, though not yet fully understood.

Introduction

In an earlier paper on the systematic classification of topotactic reactions (1), we have stated that the formation of a solid product in a small number of defined, but not crystallographically equivalent, orientations can be treated as the simultaneous occurrence of several different topotactic reactions. This is still valid, although the wording of the definition of topotaxy has been slightly modified since to include solid state polymerizations and phase transformations (2):

A process is called topotactic, if its solid product is formed in one or several crystallographically equivalent orientations relative to the parent crystal as a consequence of a chemical reaction or a solid state transformation, and if it can proceed throughout the entire volume of the parent crystal.

¹ Author to whom correspondence should be addressed.

Simultaneous occurrence of several competing structural reaction mechanisms is by no means common, but the study of such processes may give important insights into the origins of the phenomenon of topotaxy. In a short note, it has been reported briefly that the dehydration of potassium metavanadate monohydrate, $\text{KVO}_3 \cdot \text{H}_2\text{O}$ is such a case (3).

The present paper presents new results of much more detailed observations on this specific reaction.

Experimental

Preparation of Potassium Metavanadates

A saturated solution of potassium vanadate was prepared by adding solid KOH to an aqueous suspension of V_2O_5 (Merck, purum) until a pH of 6.5 was reached (if this value was exceeded, it could be reduced by adding small amounts of V_2O_5). After filtra-

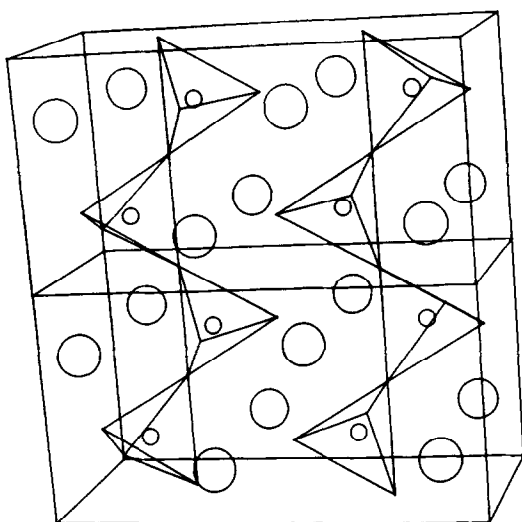


FIG. 1. Crystal structure of KVO_3 (small circles, vanadium; corners of tetrahedra in chains parallel to $[001]$, oxygen; large circles, potassium).

tion, the pH was brought to 7.0 by addition of aqueous KOH. This had to be repeated several times, as the hydrolysis equilibrium is only slowly attained.

$KVO_3 \cdot H_2O$. Slow evaporation (more than 30 days) of the above solution at ambient temperature produced single crystalline needles of $KVO_3 \cdot H_2O$ up to 3 mm in length.

KVO_3 . Polycrystalline KVO_3 powder was obtained by faster evaporation at slightly elevated temperatures (30–50°C). The products were characterized by com-

parison of their X-ray diffraction patterns with literature data (4, 5).

X-Ray Diffraction

For powder X-ray diffraction, a Guinier IV-camera (Nonius Delft) with $CuK\alpha_1$ radiation was used, KCl being added to the sample as internal standard. Relative intensities were measured with a Joyce-Loebl

TABLE II
X-RAY POWDER DIFFRACTION DATA OF
 $KVO_3 \cdot H_2O$

2θ	$d_{obs.}$	$d_{calc.}$	I/I_0 [%/°]	hke
12.65	6.992	6.981	1000	101
17.00	5.211	5.206	72	102
22.75	3.905	3.902	257	201
25.00	3.559	3.556	165	011
25.50	3.490	3.491	361	202
27.30	3.264	3.260	402	111
28.55	3.124	3.124	361	104
29.50	3.025	3.024	557	203
29.65	3.010	3.008	371	112
31.30	2.855	2.854	742	013
32.70	2.736	2.734	206	210
33.20	2.696	2.694	196	113
33.40	2.680	2.679	639	211
33.60	2.665	2.663	216	301
34.40	2.605	2.603	93	204
35.40	2.533	2.535	103	212
35.55	2.523	2.521	82	302
38.45	2.339	2.338	216	213
39.90	2.257	2.255	268	006
41.50	2.174	2.174	51	106
42.45	2.128	2.126	82	214
43.40	2.083	2.081	62	312
44.40	2.039	2.037	51	400
46.50	1.951	1.951	93	402
47.20	1.924	1.924	62	215
48.30	1.883	1.881	93	107
49.05	1.856	1.857	165	403
49.40	1.843	1.843	773	020
51.20	1.783	1.782	464	121
51.65	1.768	1.768	72	411
52.55	1.740	1.740	124	216
52.70	1.735	1.735	82	306
53.80	1.702	1.702	62	315
54.75	1.675	1.675	155	117
55.05	1.667	1.667	62	221
56.40	1.630	1.630	155	222
58.05	1.588	1.588	175	124

TABLE I

UNIT CELL PARAMETERS OF KVO_3 AND $KVO_3 \cdot H_2O$

Compound	Literature	Experiment (this work)
KVO_3 orthorhombic	(5)	
	$a = 5.176 \pm 0.002 \text{ \AA}$	$a = 5.185 \pm 0.004 \text{ \AA}$
	$b = 10.794 \pm 0.003 \text{ \AA}$	$b = 10.814 \pm 0.008 \text{ \AA}$
	$c = 5.680 \pm 0.002 \text{ \AA}$	$c = 5.692 \pm 0.004 \text{ \AA}$
$KVO_3 \cdot H_2O$ orthorhombic	(4)	
	$a = 8.151 \pm 0.008 \text{ \AA}$	$a = 8.150 \pm 0.004 \text{ \AA}$
	$b = 3.697 \pm 0.004 \text{ \AA}$	$b = 3.686 \pm 0.002 \text{ \AA}$
	$c = 13.586 \pm 0.010 \text{ \AA}$	$c = 13.532 \pm 0.006 \text{ \AA}$

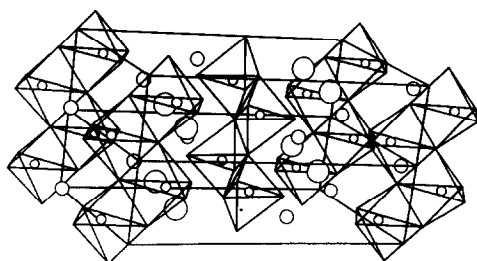


FIG. 2. Crystal structure of $KVO_3 \cdot H_2O$ (small circles, vanadium; corners of trigonal bipyramids in chains parallel to $[010]$, oxygen; medium circles, potassium; large circles, water).

double beam microdensitometer. For single crystal X-ray diffraction, Precession and Weissenberg methods with $MoK\alpha$ and $CuK\alpha$ radiation, respectively, were applied.

Thermal Decomposition

The thermal decomposition of the hydrate was followed continuously by thermogravimetry on a Perkin-Elmer thermogravimetric system TGS-2 and on a Mettler Thermoanalyzer TA-1. Continuous heating X-ray diffraction of powders was performed on a Huber camera system 600, and enthalpy measurements were made on a Perkin-Elmer DSC-2 apparatus.

Morphology

Morphological investigations were made with a stereo magnifier mounted on a Met-

TABLE III
TOPOTACTIC ORIENTATION RELATIONS^a

A.	$(100)_H//$	(100)	$(001)_H//$	(010)
B.	$(100)_H//$	(010)	$(001)_H//$	(100)
C.	$(100)_H// \pm 60^\circ$	(010)	$(001)_H// \pm 60^\circ$	(100)
D.	$(100)_H//$	(021)	$(001)_H//$	(100)
E.	$(100)_H// \pm 56^\circ$	(021)	$(001)_H// \pm 56^\circ$	(100)

^a $(hke)_H$ refers to the hydrate, (hke) to $KVO_3 \cdot \pm 60^\circ$ means that the plane of KVO_3 is rotated by 60° relative to the hydrate plane.

tlar FP-52 heating device, and with a scanning electron microscope Stereoscan S-4 (Cambridge Instruments Ltd.).

The Dehydration Reaction

Thermogravimetric measurements were made under varying conditions and gave the following results.

At ambient pressure in flowing nitrogen (10 ml/min) with a heating rate of $10^\circ C/min$, the decomposition occurred in one single step, the weight loss corresponding to one molecule of water per formula unit. The water release initiated at $75^\circ C$ and was completed at $130^\circ C$. The weight then remained unchanged up to $200^\circ C$.

Isothermal decomposition at room temperature under a pressure of 10^{-2} Torr led to a continuous loss of the water within 4 to 6 hr. Crystals kept at room temperature

TABLE IV
EXPERIMENTAL CONDITIONS AND TOPOTAXY DATA

Experiment	Pressure (Torr)	Temperature ($^\circ C$)		Heating period (hr)	Heating rate ($^\circ C/hr$)	Orientation (refer to Table III)
		Start	End			
1	760	25	150	24	~ 5	A,D
2	760	160	160	Fast (2 hr isothermal at $160^\circ C$)	—	B,D
3	20	25	150	72	~ 2	D,E
4	10^{-3}	-196	160	96	~ 4	B,C

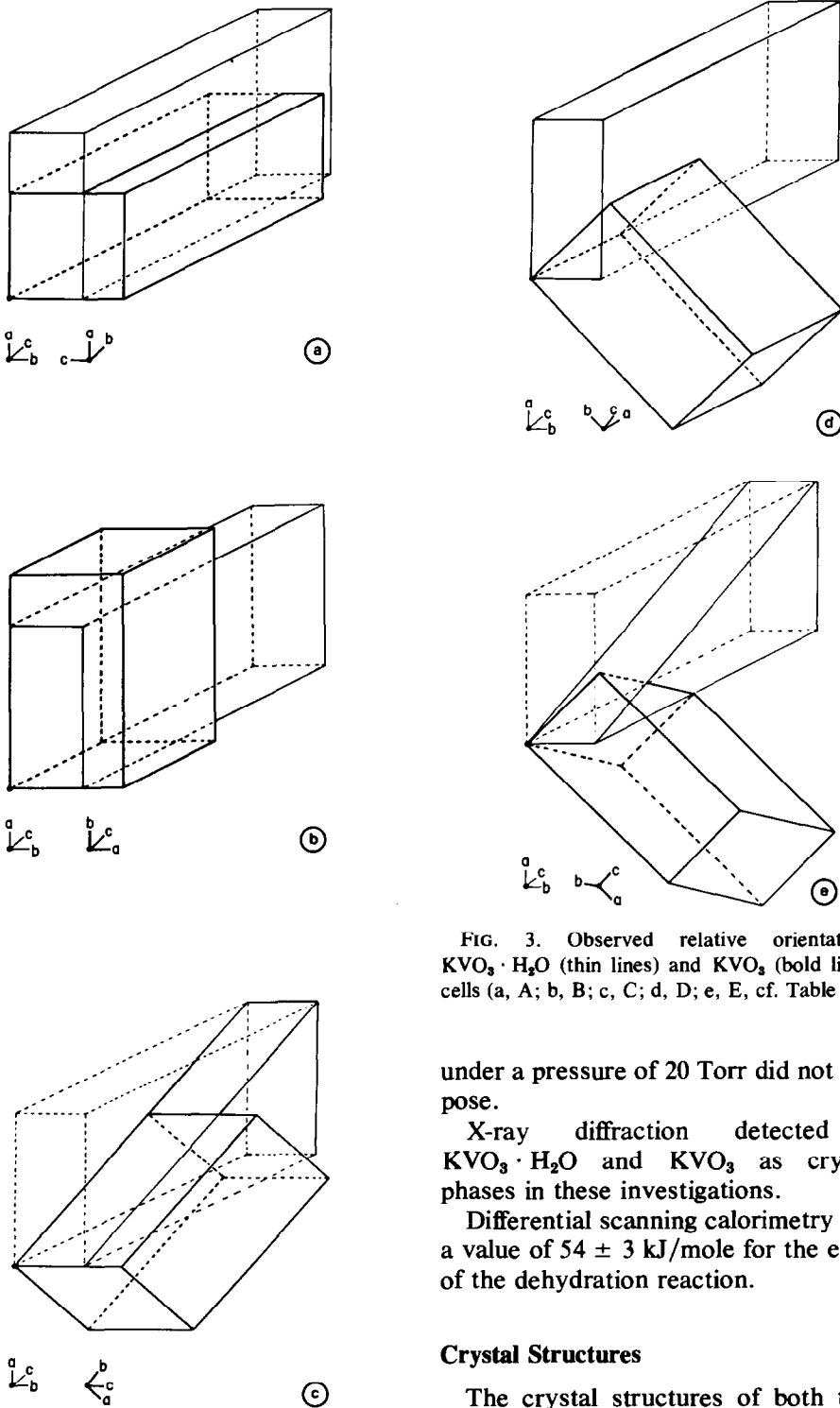


FIG. 3. Observed relative orientations of $\text{KVO}_3 \cdot \text{H}_2\text{O}$ (thin lines) and KVO_3 (bold lines) unit cells (a, A; b, B; c, C; d, D; e, E, cf. Table III).

under a pressure of 20 Torr did not decompose.

X-ray diffraction detected only $\text{KVO}_3 \cdot \text{H}_2\text{O}$ and KVO_3 as crystalline phases in these investigations.

Differential scanning calorimetry yielded a value of 54 ± 3 kJ/mole for the enthalpy of the dehydration reaction.

Crystal Structures

The crystal structures of both the hy-

drated and the anhydrous potassium metavanadates are characterized by vanadate chains. Whereas KVO_3 contains chains of corner sharing tetrahedra (5), as represented by Fig. 1, $\text{KVO}_3 \cdot \text{H}_2\text{O}$ is built up from chains of edge sharing trigonal bipyramids (4), shown in Fig. 2. The lattice constants of our samples, obtained from least-squares refinements of X-ray powder diffraction patterns, are in good agreement with literature data (Table I).

The completely indexed X-ray powder diffraction diagram of $\text{KVO}_3 \cdot \text{H}_2\text{O}$, not yet reported in the literature, is given in Table II.

Orientation Relations

Single crystal X-ray diffraction photographs from one and the same crystal before, after partial, and after complete dehydration were used to determine the relative orientations of the two phases under varying dehydration conditions.

Invariably, more than one crystallographically nonequivalent sets of orientation relations were found in any individual crystal, in most crystals two sets being predominant.

Topotactic orientation relations observed are given in Table III. Relations C and E occur furthermore in two twin-related positions each. The occurrence of the various orientation relations was found to depend on the reaction conditions, although no conditions could be specified in which only one single product orientation appeared. The experimental conditions and their respective, reproducibly observed topotaxy data are listed in Table IV.

Product Morphology

The pseudomorphs resulting from crystals submitted to the different dehydrating conditions (cf. Table IV) and producing dif-

ferent product orientations varied only slightly in their morphology. Their common features are more or less pronounced cracks parallel to the needle axes. They are most pronounced for experimental condition 4 and least developed under conditions 1 and 2. For condition 3, additional cracking perpendicular to the needle axis was observed.

Geometrical Interpretation

A geometrical illustration of the observed product orientations A to E (cf. Table III) is represented by Figs. 3a through e. From a simple comparison of the crystal structures of $\text{KVO}_3 \cdot \text{H}_2\text{O}$ and of KVO_3 , it might be expected that the anionic chains as dominating structural motive could essentially be conserved throughout the dehydration reaction. This implies that one V-O bond per formula unit must be broken, as is illustrated in Fig. 4, and the chain stretched by 54% from a periodicity of 3.70 Å to one of 5.68 Å.

As has been stated earlier (3), the occurrence of topotactic reactions is strongly related to both the minimization of the number of strong chemical bonds, which have to be broken, and to the minimization of the displacements of those atoms which remain in the product. The above postulated geometrical reaction mechanism completes the

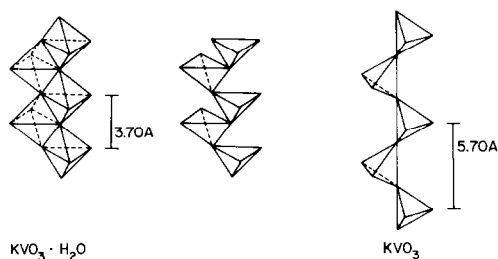


FIG. 4. Topological relation of chains of edge sharing trigonal bipyramids in $\text{KVO}_3 \cdot \text{H}_2\text{O}$ and of chains of corner sharing tetrahedra in KVO_3 , showing the need of breaking one V-O bond per formula unit when going from one to the other.

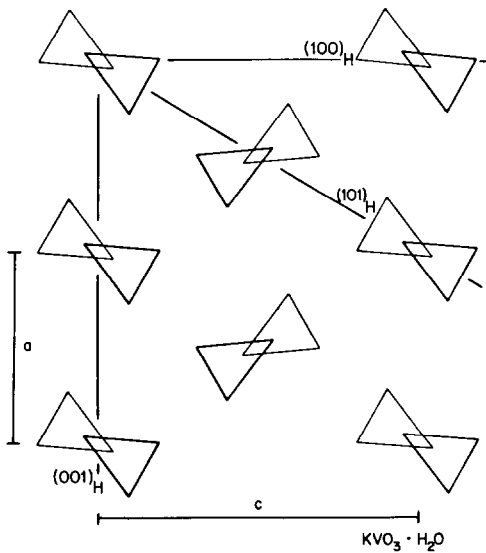


FIG. 5. Projection $[010]_H$ of the $KVO_3 \cdot H_2O$ structure (K^+ and H_2O omitted; VO_3^- alternately in 0 and $b/2$). Traces of the planes $(100)_H$, $(101)_H$, and $(001)_H$ are indicated.

first requirement, one bond out of five being the minimal number possible of bonds being broken when going from a trigonal bipyramidal to a tetrahedral coordination. However, the second condition appears to be

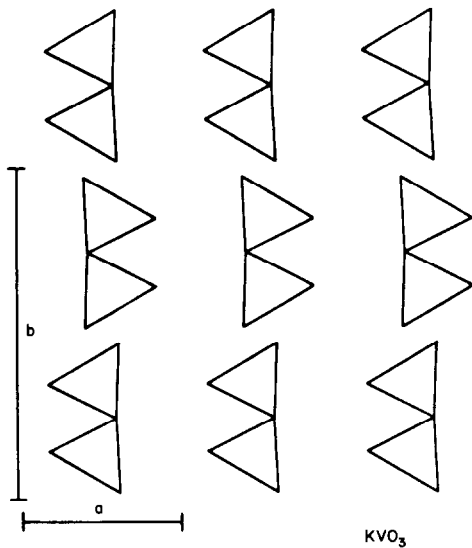


FIG. 6. Projection $[001]$ of the KVO_3 structure (K^+ omitted).

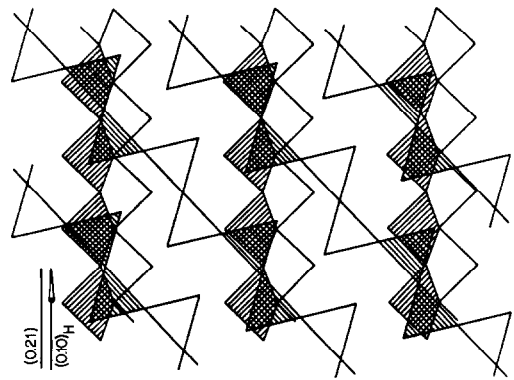


FIG. 7. Overlay of schematic projections $[001]_H$ of $KVO_3 \cdot H_2O$ and $[100]$ of KVO_3 in experimentally found orientation relation D. Shaded polyhedra may keep their position almost unaltered in the transformation from one structure to the other.

hardly fulfilled in view of the elongation of chains by more than 50%!

Comparison with the experimental results shows that the orientation of the anionic chains, $[010]_{hydrate}$ and $[001]_{vanadate}$ respectively, is indeed conserved in the orientation relations A, B, and C, but not in D and E. These two latter cases will be dealt with separately later. To illustrate the origin of three different product orientations, in all of which the anionic chains are con-

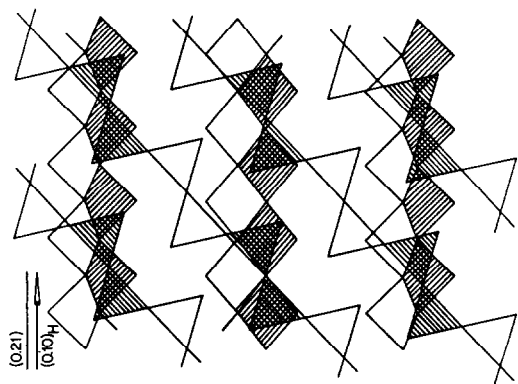


FIG. 8. Overlay of schematic projections onto $(101)_H$ of $KVO_3 \cdot H_2O$ and onto (100) of KVO_3 in experimentally found orientation relation E. Shaded polyhedra may keep their position almost unaltered in the transformation from one structure to the other.

served and expanded by the same amount, the projections of the crystal structures involved, seen along these chains, have to be compared (Figs. 5 and 6). (In these figures, the structures are simplified as much as possible, only the contours of the coordination polyhedra of vanadium being drawn and all other atoms omitted.)

From these figures, it becomes evident, that the chains have not only to be stretched, but also rotated around their axes to assume the position required in the product structure. If larger movements of integral chains perpendicular to their direction of elongation are excluded, this rotation can only occur in three possible ways: resulting in a position of $(100)_{\text{vanadate}}$ parallel to $(100)_{\text{hydrate}}$, to $(001)_{\text{hydrate}}$, or to $(101)_{\text{hydrate}}$, the latter furthermore being in a twin relationship to its equivalent possibility $(10\bar{1})_{\text{hydrate}}$. In fact, these three possibilities correspond to the experimentally found orientations A, B, and C, the latter occurring in two twin-related positions.

The explanation of the occurrence of two further product orientations (D and E) is less straightforward.

In order to interpret orientation D, the projections $[001]_{\text{hydrate}}$ and $[100]_{\text{vanadate}}$ have

Interchain distance in $(100)_{\text{hydrate}} = 7.92 \text{ \AA}$ (cf. experimentally found orientation E),

in $(001)_{\text{hydrate}} = 8.15 \text{ \AA}$ (cf. experimentally found orientation D),

e.g., in $(100)_{\text{hydrate}} = 13.6 \text{ \AA}$ (next shortest distance, not found experimentally).

Therefore, from geometrical considerations alternative possibilities for chain rearrangement can be ruled out and have, in fact, not been observed.

Conclusions

The earlier statement (3) that topotactic processes follow the tendencies to (a) mini-

to be compared. In a simplified representation similar to that used above, these two projections can directly be superimposed (Fig. 7). It can be seen that a reconstruction of the individual chains, by breaking the initial chains and forming new links to neighboring chains, yields an arrangement of the atoms, the formation of which involves very little atomic displacements, but the number of V-O bonds broken is increased by 25% to 1.25 bonds/formula unit.

The interpretation of orientation E can be explained by very similar arguments, superposing projections onto $(101)_{\text{hydrate}}$ and onto $(100)_{\text{vanadate}}$. The resulting Fig. 8 is very similar to Fig. 7. The angle between the planes $(101)_{\text{hydrate}}$ used for Fig. 8 and $(100)_{\text{hydrate}}$ used for Fig. 7 is 59° , well comparable with the experimentally found value of 56° (cf. Table III). For orientation E, a twin-related orientation with $(10\bar{1})_{\text{hydrate}}$ instead of $(101)_{\text{hydrate}}$ is expected and indeed experimentally found. Inspection of Fig. 5 shows that no other planes allow for such an easy rearrangement of the chains as in $(101)_{\text{hydrate}}$ and in $(001)_{\text{hydrate}}$, the distances between neighboring chains being much longer in all other possible orientations:

mize the number of strong chemical bonds to be broken, and (b) keep the atomic displacements minimal, was based on numerous examples of topotaxy (1). In most of these, the implications of these two tendencies work in parallel and therefore the result is usually obvious.

In the presently described reaction, however, these two "driving forces" work in

opposite directions. From the five different product orientations (which are crystallographically nonequivalent), three can be explained by a mechanism, which requires the minimum of one V–O bond to be broken per formula unit, whereas the two others require breaking of 1.25 strong V–O bonds/formula unit. On the other hand, in these latter two, the atomic rearrangement can be achieved by minimal displacements, whereas the first three require considerable stretching of anionic chains by more than 50% of their original length. It is therefore an illustrative example of the two tendencies. Others than the observed five product orientations can be ruled out from geometrical reasons, except for statistical arrangement of the product crystallites due to a nontopotactic reaction mechanism.

The influence of the reaction conditions on the occurrence of specific reaction mechanisms is difficult to understand. Whereas dehydration under atmospheric pressure yielded chain expansion as well as reconstruction simultaneously (Table IV, experiments 1 and 2), slow reaction rates at reduced pressures yielded only chain reconstruction at 20 Torr (experiment 3), and only chain expansion at 10^{-2} Torr (experiment 4). Qualitatively, it may be argued

that the higher water vapor pressure in experiment 3 reduces the rate of water removal from between the planes, intensifying the interaction between neighboring chains within one and the same plane, whereas the high mobility of the water in the lattice at the lowest pressure favors the adoption of the new structure by a rearrangement within one and the same chain. The fact that in experiment 3 no chains are conserved as such agrees with the morphological result of visible cracks perpendicular to the chain direction. However, the influences of experimental conditions on the reaction mechanism discussed above are not yet fully understood.

References

1. J. R. GÜNTER AND H. R. OSWALD, *Bull. Inst. Chem. Res. Kyoto Univ.* **53**, 249 (1975).
2. H. R. OSWALD AND J. R. GÜNTER, in "1976 Crystal Growth and Materials" (E. Kaldis and H. J. Scheel, Eds.), p. 416. North Holland, Amsterdam (1977).
3. J. R. GÜNTER AND H. R. OSWALD, *Z. Kristallogr.* **142**, 457 (1975).
4. C. L. CHRIST, J. R. CLARK, AND H. T. EVANS, *Acta Crystallogr.* **7**, 801 (1954).
5. F. C. HAWTHORNE, *J. Solid State Chem.* **22**, 157 (1977).